

Exhibit A.

Sensing and compensation of femtosecond waveform distortion induced by all-order polarization mode dispersion at selected polarization states

Houxun Miao and Andrew M. Weiner

Purdue University, West Lafayette, Indiana 47907, USA

Carsten Langrock, Rostislav V. Roussev, and Martin M. Fejer

E.L. Ginzton Laboratory, Stanford University, Stanford, California 94305, USA

Received September 19, 2006; accepted November 1, 2006;

posted November 14, 2006 (Doc. ID 75199); published January 26, 2007

We demonstrate full characterization of femtosecond pulse distortion induced by all-order polarization mode dispersion (PMD) at selected polarization states via second-harmonic generation (SHG) frequency-resolved optical gating (FROG) measurements at an average power of under 28 nW. By applying the inverse of the measured spectral phase via a programmable pulse shaper, we compress the distorted pulses from more than 3 ps to nearly bandwidth-limited durations of less than 500 fs. Our results show that SHG FROG measurements performed by using fiber-pigtailed aperiodically poled lithium niobate waveguides can serve as a robust and sensitive tool for characterization of PMD-induced spectral phase. © 2007 Optical Society of America

OCIS codes: 060.2330, 260.5430, 320.7100, 320.5540.

Polarization mode dispersion (PMD) is considered one of the major obstacles for the development of ultrahigh-capacity telecommunication systems. PMD arises from the random birefringences in single-mode fibers due to the imperfection in the cylindrical symmetry.¹ This results in time-stochastic and wavelength-dependent variation of the states of polarization (SOPs) and delays, which may degrade the system capacity. Generally, PMD is represented by a 3×1 vector in Stokes space, and the frequency dependence of PMD is expanded in terms of successive frequency derivatives of this PMD vector. Most current PMD compensation work is restricted to the low-order (first- and second-order) PMD approximation.^{2,3} However, as the bandwidth of telecommunication systems increases, all-order PMD effects become increasingly important.⁴ All-order PMD results in a complicated wavelength-dependent SOP and wavelength- and polarization-dependent delay (equivalent to spectral phase). In previous work^{5,6} we demonstrated experimental wideband all-order PMD compensation by applying ultrafast pulse-shaping techniques.⁷ To achieve all-order PMD compensation, we first rotated the distorted SOP spectrum to a fixed linear state on a wavelength-by-wavelength basis through a specially designed pulse shaper and then applied the inverse of the estimated spectral phase via a phase-only pulse shaper. Our estimate of the spectral phase was obtained by measuring the temporal intensity by cross correlation and then applying the Gerchberg-Saxton algorithm. However, owing to the complexity of the all-order PMD-induced pulse distortion and the limits of the Gerchberg-Saxton algorithm, an iterative measure-compensate-measure procedure was necessary, which lacked the robustness that will be needed for real applications.

In this Letter we explore ultralow-power second-harmonic generation (SHG) frequency-resolved optical gating⁸⁻¹⁰ (FROG) for accurate characterization of spectral phase distortions induced by all-order PMD. Since our FROG setup is polarization sensitive, the PMD-induced frequency-dependent SOPs must be fixed to a specified state. Although this may be performed by using the wavelength-by-wavelength polarization rotation apparatus of Ref. 5, instead here we simply use two polarization controllers (PCs) and a polarizer to select single-polarization slices of the distorted waveform (see Fig. 1) and then perform FROG measurement and spectral phase correction at the selected slices. In this way we report full characterization of all-order PMD-induced femtosecond pulse distortion at selected SOP slices. By correcting the measured spectral phase via a phase only pulse shaper, the distorted pulses at the selected SOP slices are compressed from several picoseconds to bandwidth-limited durations of less than 500 fs, without any need for iteration. Note that the pulses used in this work are significantly shorter than those (~800 fs) in Ref. 6, while the durations of the distorted pulses are close to those in Ref. 6. Our results show that FROG is substantially more robust than the Gerchberg-Saxton algorithm for characterization of spectral phase distortions induced by all-order PMD.

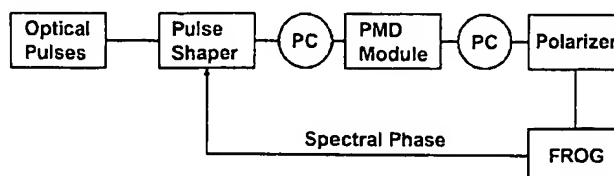


Fig. 1. Experimental setup. PC, polarization controller.

Another advantage of our FROG measurement is the extremely high sensitivity (the minimum peak-power-average-power product) of $2.0 \times 10^{-6} \text{ mW}^2$, which allows high-quality pulse measurements at nanowatt to tens of nanowatts average power for a laser at a 50 MHz repetition rate.¹⁰ In the present paper all measurements are performed at an average power under the 28 nW level. Such high measurement sensitivity is very important for fiber optic applications, for example, since powers are typically low (especially after fiber transmission). Our results are obtained by using a fiber-pigtailed aperiodically poled lithium niobate waveguide device.^{10,11} As in our group's previous work,^{9,10} the strong nonlinear interaction within the waveguide structure contributes to the unprecedented sensitivity, while the chirped poling period broadens the phase matching response (to $\sim 25 \text{ nm}$) to accommodate the full bandwidth of the femtosecond pulses.

Figure 1 shows our experimental setup. A passively mode-locked fiber ring laser followed by a bandpass filter ($\sim 10 \text{ nm}$ FWHM) together are used to produce $\sim 360 \text{ fs}$ optical pulses with a $\sim 50 \text{ MHz}$ repetition rate and 1550 nm center wavelength. The pulses are relayed into a fiber-coupled reflective Fourier-transform pulse shaper, which incorporates a two-layer, 128-element liquid crystal modulator array to apply spectral phase. The two layers of the liquid crystal modulator are programmed in common mode, resulting in a polarization-insensitive phase-only modulation functionality. The output of the pulse shaper is launched into a homemade PMD emulator consisting of eight sections of polarization maintaining fiber spliced at various angles. The distorted pulses are then transmitted through a polarizer into the measurement setup. Since the average differential group delay ($\sim 1.3 \text{ ps}$) of the PMD module is much greater than the pulse width, strong all-order PMD effects are present, which cause complicated variation of the SOP with frequency. This leads to reshaping of the spectrum after the polarizer. With two PCs, one placed before and one after the PMD module, we can select arbitrary polarization slices for spectral phase characterization and correction. In our initial experiment the chromatic dispersion of the PMD module is not precompensated. The phase correction is run in precompensation mode. The same results can be achieved in postcompensation mode.

Figures 2 and 3 show a first trial in which we perform FROG measurements on a selected polarization slice. The quadratic spectral phase is caused mainly by the chromatic dispersion, while the complexity of the pulse in the time domain is due to all-order PMD effects. By applying the inverse of the measured spectral phase, the pulse is compressed dramatically from more than 3 ps (at 10% intensity level) in duration to 484 fs (FWHM), which is close to bandwidth limited. Both PMD- and chromatic-dispersion-induced distortions are compensated almost completely.

We then keep the applied spectral phase with the phase-only pulse shaper and adjust the input and output PCs to select another experimental trial. In this case the chromatic dispersion has been fully

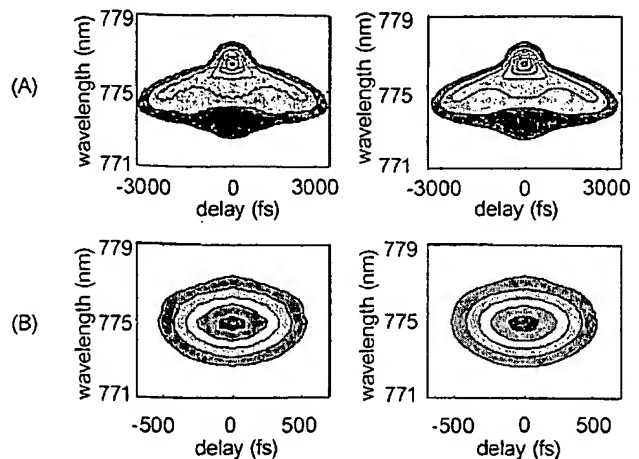


Fig. 2. (Color online) Measured (left) and retrieved (right) FROG traces: (A) before compensation, (B) after compensation.

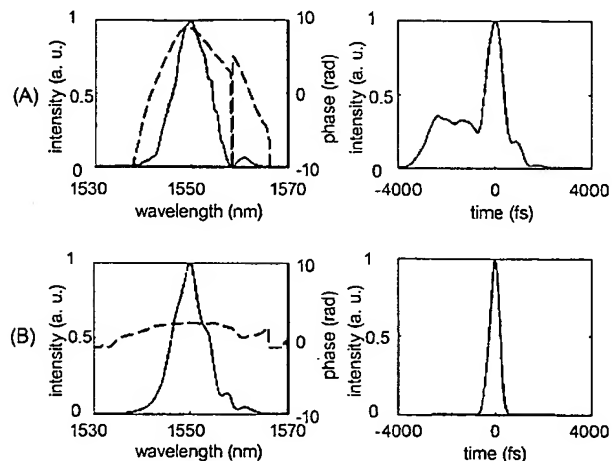


Fig. 3. Retrieved pulses depicted in the frequency and time domains. Solid curves, retrieved intensity profiles; dashed curves, retrieved spectral phase profiles. (A) Before compensation, (B) after compensation.

compensated in the previous trial. The pulse distortion is caused by the difference between the PMD-induced spectral phases for the two experimental trials. The experimental results are shown in Figs. 4 and 5. The pulse is stretched to about 2 ps by the PMD effects and compensated to a bandwidth-limited pulse of 400 fs .

To check the generality of our technique, we concatenate the original PMD module with a second PMD module (again consisting of eight spliced PM fiber segments with $\sim 1.3 \text{ ps}$ average differential group delay). The PMD modules are connected via a PC. We perform the measurement and correction process at a polarization slice selected to exhibit a relatively complex spectrum after the polarizer. Figure 6 shows the measured pulses before and after correction. The pulse is compressed to a 387 fs bandwidth-limited pulse after correction. In Fig. 6(B) the power spectrum is somewhat smoothed out by the FROG retrieval program.

It is worth noting that PMD-induced spectral reshaping after the polarizer accounts for the small pulse width differences between the initial pulse and

the pulses after correction, while the FROG retrieval algorithm accounts for the slight differences of the spectra before and after compensation. Since spectral phase plays the primary role in pulse distortion, the

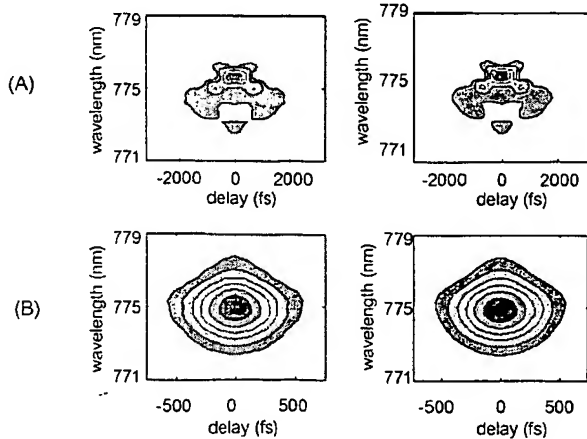


Fig. 4. (Color online) Measured (left) and retrieved (right) FROG traces: (A) before compensation, (B) after compensation.

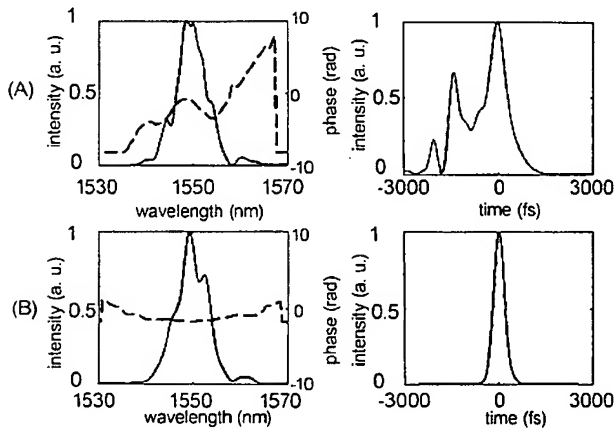


Fig. 5. Retrieved pulses depicted in the frequency and time domains. Solid curves, retrieved intensity profiles; dashed curves, retrieved spectral phase profiles. (A) Before compensation, (B) after compensation.

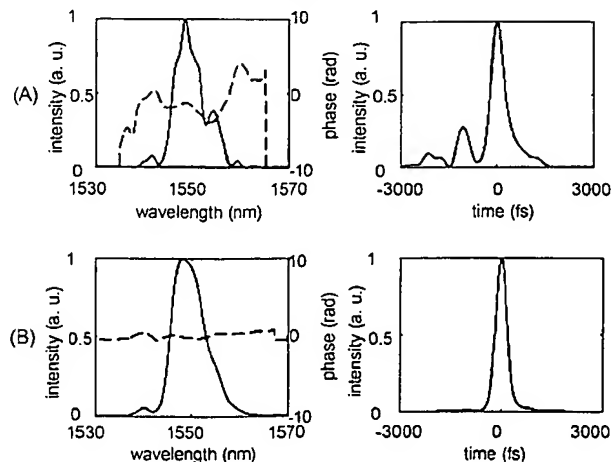


Fig. 6. Measured pulses in the frequency and time domains. Solid curves, retrieved intensity profiles; dash curves, retrieved spectral phase profiles. (A) Before compensation, (B) after compensation.

slight difference in retrieved spectra is not a significant problem.

With the two concatenated PMD modules, we adjusted the PCs to select several other output signals and in each case performed spectral phase correction. In all cases, we achieved nearly Fourier-transform-limited pulses immediately after the phase measurement and correction process, with no need for iteration. All FROG measurements were made at under 28 nW average power, with FROG errors of 0.008 or below, indicating good quality in waveform retrieval.

In conclusion, we have demonstrated full characterization of all-order PMD-induced femtosecond waveform distortion at selected polarization slices via SHG FROG measurements at ultralow power. We have also achieved complete compensation of the distortion at the selected polarization slices by using the FROG data to control a programmable spectral phase shaper. Our results show that ultralow-power SHG FROG has the potential to serve as a robust and highly sensitive tool for pulse characterization in short pulse, all-order PMD compensation research. Note that our current work does not yet demonstrate full all-order PMD compensation. In our future work, we intend to employ FROG for spectral phase sensing in complete all-order PMD compensation experiments involving first wavelength-parallel polarization correction⁵ followed by our current apparatus for spectral phase compensation.

The authors acknowledge Shang-Da Yang, Li Xu, and Daniel Leaird for their contribution. This work was funded by the National Science Foundation under grants 0501366-ECS and 0401515-ECS. H. Miao's e-mail address is hmiao@purdue.edu

References

1. H. Kogelnik, R. M. Jopson, and L. E. Nelson, in *Optical Fiber Telecommunications IVB—Systems and Impairments*, I. P. Kaminow and T. Li, ed. (Academic, 2002), p. 723.
2. Q. Yu, L.-S. Yan, Y. Xie, M. Hauer, and E. Willner, *IEEE Photon. Technol. Lett.* **13**, 863 (2001).
3. P. B. Phua and H. A. Haus, *IEEE Photon. Technol. Lett.* **14**, 1270 (2002).
4. H. Miao and C. Yang, *IEEE Photon. Technol. Lett.* **16**, 2475 (2004).
5. M. Akbulut, A. M. Weiner, P. Cronin, and P. J. Miller, *Opt. Lett.* **29**, 1129 (2004).
6. M. Akbulut, A. M. Weiner, and P. J. Miller, *Opt. Lett.* **30**, 2691 (2005).
7. A. M. Weiner, *Rev. Sci. Instrum.* **71**, 1929 (2000).
8. R. Trebino, *Frequency-Resolved Optical Gating: the Measurement of Ultrashort Laser Pulses* (Kluwer Academic, 2000).
9. S. Yang, A. M. Weiner, K. R. Parameswaran, and M. M. Fejer, *Opt. Lett.* **30**, 2164 (2005).
10. H. Miao, A. M. Weiner, S. Yang, C. Langrock, R. V. Roussev, and M. M. Fejer, *15th International Conference on Ultrafast Phenomena* (Optical Society of America, 2006), paper WC2.
11. J. Huang, X. P. Xie, C. Langrock, R. V. Roussev, D. S. Hum, and M. M. Fejer, *Opt. Lett.* **5**, 604 (2006).